# An automated light scattering system scanning in two spherical angles

Xin Wen,[a] Mark J. Schnitzer, and Robert B. Meyer
*The Martin Fisher School of Physics, Brandeis University, Waltham, Massachusetts 02254*

(Received 29 November 1989; accepted for publication 11 April 1990)

We have designed and built a light scattering system that can detect scattered light in two spherical angles with scanning ranges more than 270° about the vertical axis and 100° about a horizontal axis. The detector and the sample holder are automated by high-precision stepping motors with a minimal angular increment 0.01° or 0.02°. A novel modular design in the detector allows the experimenter to examine the image of the scattering object and the direction of the scattered light while the detector is fixed at the measurement position. The angular resolution of the system is smaller than 0.19° in both azimuthal and polar directions. This setup has been successfully applied to study the static and dynamic properties of the ordered phases in colloidal solutions.

## I. INTRODUCTION

Laser light scattering is a useful experimental technique[1,2] for studying structural and dynamic properties of the phases formed in suspensions of colloidal particles. In the many designs of light scattering systems previously reported, the detector is designed either to be fixed at 90° (Ref. 3) or at as many as 18 different angles,[4] or to be rotated in an angular range.[5–7] However, the rotation motion of the detector in all these designs is restricted in one scattering plane.

A subject of great current interest is the physical properties of the crystalline and liquid crystalline phases formed by colloidal particles in solutions. These ordered phases by definition are anisotropic in space. In the crystalline phase, the particles are distributed in crystalline planes with different orientations. In the liquid crystalline phases, the anisotropic particles are aligned in a preferred orientation and in some cases form periodic structures in one or two dimensions. To study such anisotropic structures, it is necessary to analyze the scattered light as a function of both spherical angles. Such a task is often difficult for a conventional light scattering device whose detection geometry is limited in one scattering plane. It requires combined rotations of the sample and the detector, which changes illumination conditions in the sample and may damage delicate colloidal structures. For this reason, we designed and built a light scattering system that can detect scattered light over wide angular ranges in two spherical angles for each fixed sample geometry.

In our light scattering system illustrated in Figs. 1(a), 1(b), and 1(c), the sealed sample and the scaled entrance end of the detector are immersed in a solvent that matches the refractive index of the sample solution, so that the refractive effects at the sample boundaries are minimized. For taking large amounts of data at many angular positions, the detector assembly and the sample are rotated by high-precision stepping motors under computer control. A multipurpose detector system allows the observation of the scattering object and the spatial and angular filtering of the scattered light while the detector is fixed at the measurement position. A minimum number of adjustments are needed to achieve alignment of the system. The setup was found to meet all the design requirements when it was applied to the study of the smectic A liquid crystalline phase formed by rodlike colloidal particles.[11]

In the following, we will describe in sequence the sample holding system (Sec. II), the detection assembly (Sec. III), automation of the detector and the sample (Sec. IV), system alignment (Sec. V), and calibration and experimental performance of the setup (Sec. VI).

## II. SAMPLE HANDLING

The sample solution is typically contained in a 1-mm-diam quartz capillary tube with a wall thickness of about 10 $\mu$m. The sample is held from above by a rod attached to a goniometer ($G$ in Fig. 1). The goniometer (Charles Supper Co.) consists of 3D translational stage on two rotational stages, which allows manual adjustments of the orientation and the position of the sample capillary. The goniometer can also be rotated about a vertical axis by Motor2 that is mounted on the platform above the tank. The refractive distortions of the incident and scattered light at the walls of the sample capillary are minimized by immersing the sample in an index-matching solvent contained in a 10-in.-diam cylindrical tank. The incident laser beam is focused by a lens outside of the tank and enters the tank through the entrance window ($E$ in Fig. 1). The scattered light from the sample is received by the detector entrance window [$E1$ in Figs. 1(b) and 1(c)].

## III. THE DETECTION SCHEME

There are five main requirements on the design of the detection assembly in our light scattering system. First, since the entrance end of the detector is immersed under an index-matching solvent, the scattered light needs to be transported from there to the detection device. Second, vertical and horizontal scattering polarizations must be selected. Third, the detector should allow the experimenter to observe the sample when the detector is fixed in the geometry in which the scattering light will be measured.[10] Fourth, the detector needs to perform the functions of spatial and angular filtering of the scattered light in addition to convenient observation of the sample. Last, for angular scanning, the detection process needs to be automated by motors. Due to the loading limit of the motors, the detection system should be lightweight.

[a] Department of Chemistry and Center for Material Science and Engineering, Massachusetts Institute of Technology, Cambridge, MA 02139.

 0034-6748/90/082069-04$02.00  

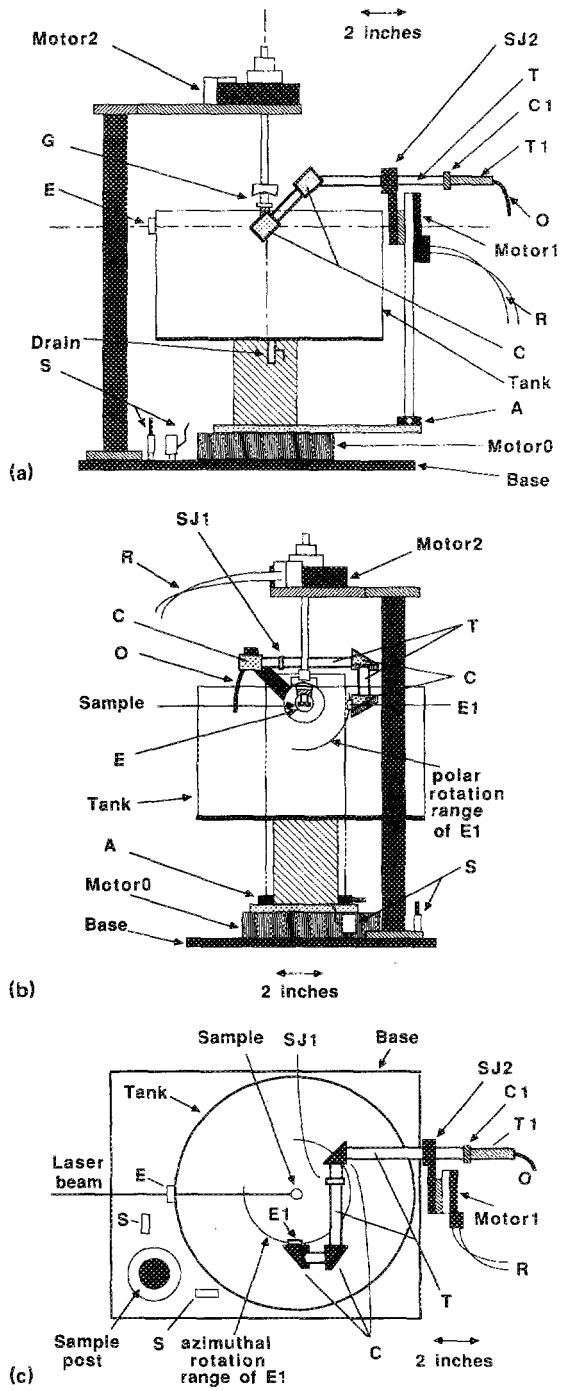


FIG. 1. The automated light scattering setup: the front view (a), the side view (b), and the top view (c). Motor0 and Motor2 have a common vertical rotational axis. Motor1 has a horizontal rotation axis. The rotation axes are illustrated by the dash-dot lines in 1(a). Motor2 and the platform holding the sample are not shown in 1(c) for clarity. Other components: *E*, the tank entrance window; *G*, the goniometer for holding samples; *E*1, the entrance window of the detector tubing; *T*, the telescoping tubing that houses the lens-and-mirror image transport system; *C*, the corner pieces on which the mirrors are mounted; *SJ*1 and *SJ*2, slip joints for aligning the position and orientation of the tubing system; *C*1, a clamp for fixing the modular detector pieces; *T*1, the modular piece for collecting data; *O*, an optical fiber; *R*, a ribbon cable for motor control; *A*, a translational stage for aligning the rotation axis of Motor1; *S*, the safety microswitches.

To meet these requirements, we designed an imaging system with lightweight brass telescope tubing of wall thickness 1/32 in. and diameters about 5/8 in. The scattered light is received by the tubing entrance window [*E*1 in Figs. 1(b) and 1(c)] that is aligned pointing to the center of the scattering sphere. The image of the scattering object is formed by a system of one lens and three mirrors housed in the tubing. The brass tubes are soldered together by three right-angle corner pieces. Each of the corner pieces holds a mirror that performs a right-angle reflection of light traveling along the tubing axis. The two mirrors nearest to the entrance window are sealed since they are sometimes immersed in solvent during an experiment. The mirror near the output end that is always in air can be detached for positioning a lens mounted inside the tubing between the top two corner pieces. The lens is chosen to form a one-to-one image of the scattering object in a plane near the outlet of the tubing system. A rotational joint (*SJ*1) is incorporated in the lens-holding tube, at a position that is always above the liquid surface. The tubing system is clamped by a slip joint (*SJ*2) to an aluminum arm that is rigidly connected to Motor1. The tubing is blackened inside with a carbon coating to absorb stray light. Other aluminum components are also anodized to a flat black in order to absorb reflections and prevent corrosion of the components that may be in contact with the index-matching solvent. The arm from Motor1 that holds the tubing system can rotate through more than 90°, without the tubing hitting the side of the tank. This allows the entrance window *E*1 to scan the polar angular range from horizontal to vertical [Fig. 1(b)]. Polarization of the scattered light is selected by a disk of sheet polarizer at the entrance widow *E*1, which can be oriented to select vertical or horizontal polarization. Note that *VV* or *VH* scattering geometry is maintained for all azimuthal and polar angles of *E*1.

For the output of the imaging system, three modular pieces were designed for observing the sample and for spatial and angular filtering of the scattered light. Any one of the modular pieces can be plugged into the exit end of the tubing. The first modular piece has along its optical axis a viewing lens focused on a plexiglass window with a cross hair at its center. In an experiment, the plexiglass window is positioned at the image plane of the scattering object. Looking through the viewing lens, one can see a clear image of the scattering object and easily select a scattering volume by moving the sample until the correct part is located at the cross hair. Removing the first modular piece, the second is put in its place. The second modular piece has on its optical axis a 250-$\mu$m-diam pinhole, a plexiglass window 10 cm behind the pinhole, and a viewing lens again focused on the plexiglass window. The pinhole is a spatial filter for selecting the scattering volume in the image plane of the sample. It is located at the cross hair of the first modular piece. The scattered light pattern from the pinhole is viewed on the plexiglass screen, which is useful for qualitative evaluation of the local angular distribution of the scattering. In experiments, a third modular piece replaces the second one and is used for collecting data. This modular piece has on its axis two 250-$\mu$m-diam pinholes 10 cm apart. The first pinhole again selects the scattering region in the sample at the image plane of the optical transport system; the second one selects the direction of the scattered light. The output light from the second pinhole is guided to a photomultiplier detector by an optical

fiber. The flexibility of the optical fiber allows the detection arm to rotate without restraint.

## IV. AUTOMATION

The entire detection system, shown in Fig. 1, is driven by stepping motors, Motor0 and Motor1, at minimum increments of 0.01° and 0.02° in the azimuthal and the polar directions respectively. Motor0 rotates an arm on which Motor1 is mounted, about a vertical axis passing through the scattering center. Motor1 rotates the detector system about a horizontal axis passing through the scattering center. As shown in Figs. 1(b) and 1(c), the rotation ranges of Motor0 and Motor1 are more than 270° and 90°, respectively. Motor2 rotates the sample in a 360° range about the same vertical axis as Motor0. The stepping motors are all controlled by a computer through a home-built interface circuit that consists of integrated stepping motor controller chips.

A safety system was built to prevent accidental collisions between the motors and other parts in the system. Microswitches (Fig. 1) were placed at each end of the rotation range of Motor0 and Motor1 (not shown for Motor1 in the figures). When a microswitch is pressed by a moving arm, the motor rotation in the direction toward the switch is inhibited and an alarm sounded.

## V. SYSTEM ALIGNMENT

The alignment of the motor axes is assisted by two auxiliary components: a taper-tipped rod, used as a pointer, and a cylindrical piece with a pin hole along its axis. The two components can be mounted on the rotation axes of Motor2 and Motor1, respectively. For aligning the axes of Motor0 and Motor2, the pointer rod is mounted on Motor2 so that its tip is near to the bottom of the tank. The pointer is aligned to the center of the tank by moving the sample post. The axes of Motor0 and Motor2 thus coincide because the center of the tank is on the Motor0 axis. Next, the laser beam is first aligned horizontally at the same height as the axis of Motor1. The laser beam is then moved in the horizontal plane so that it hits the tip of the pointer on the axis of Motor2, which has been raised to the same level. Now the laser beam intercepts the common axis of Motor0 and Motor2. Motor1 is aligned with the second auxiliary component mounted on it. By rotating Motor0 and adjusting the translation stage supporting the vertical arm that holds Motor1 (*A* in Fig. 1), Motor1 is aligned so that the laser beam passes through the central hole of the auxiliary component that is on the Motor1 axis. Finally, the rotation axis of Motor1, the laser beam, and the common rotation axis of Motor0 and Motor2 all meet at one point. This point defines the scattering center around which the motors rotate the detector.

The alignment of the detector arm is made with the tip of the pointer at the center of the detecting sphere. Loosening the two slip joints (*SJ* 1 and *SJ* 2), the optical axis of the final section of the tubing, which ends at the entrance window (*E* 1), can be properly aligned. Because of the right-angle joints, this axis is always perpendicular to the rotation axis of Motor1. *SJ* 1 allows rotation of the tubing about its axis. *SJ* 2 allows sliding of that tubing section parallel to the rotation axis as well as rotation of the tubing. The image of the pointer tip is observed with the first modular piece mounted at the output end of the image-transport tubing system. Good alignment is obtained when the image of the pointer tip always lies at the center of the cross hair in the image plane for the whole range of polar and azimuthal detection angles. The entire light scattering system is fixed on one base board so that the alignment is preserved when the system is moved.

## VI. CALIBRATION AND EXPERIMENTAL PERFORMANCE

The device was tested with a diffraction grating and has also been used to study the smectic A liquid crystalline phase formed in solutions of tobacco mosaic virus.[11] The tobacco mosaic virus (TMV) is a rodlike particle, 3000 Å in length and 180 Å in diameter. At particle concentrations 170–190 mg/ml, the smectic A phase forms in a stack of periodic layers about 3360 Å in thickness with the virus rods oriented perpendicular to the layers.

One novel feature in our detection optics design is the capability of observing the sample at the geometry at which the scattering signal is measured. In an experiment, the desired scattering volume of a sample is moved to the center of the detecting sphere using the translational and rotational stages on the goniometer. Viewing through the first modular piece, one can select a uniformly oriented crystalline or liquid crystalline domain as the sampling volume. Fixing the position of the sample, one then examines the direction of the scattered light with the second modular piece. If the direction of the scattered light is not exactly on axis, one can readjust the position and orientation of the sample with the aid of the first modular piece. Finally, with the third modular piece in place, the scattering signal is taken by step scanning the detector in the polar or the azimuthal directions and counting PMT pulses at each angular position.

The device was calibrated by scanning the Bragg scattering from a diffraction grating that was illuminated by a focused He-Ne laser beam of wavelength 6328 Å. The full angular width at half intensity of a diffraction maximum at a total scattering angle of about 90° was found to be 0.19° in both azimuthal and polar directions. The effect of stray scattering was examined by monitoring the PMT counting intensity when the diffracted beam was outside of the detection tubing or inside of the detection tube but not selected by the two pinholes in the third modular piece. We found that in the former and the latter cases the measured background scattering intensities were, respectively, at least 4 and 3 of orders-of-magnitude lower than the maximum diffraction intensity. The slightly higher background when the beam was in the tube was due to the stray scattering off the internal walls of the detection tubes.

How large a scattering volume is selected for measurement is determined by the size of the spatial filter that is the pinhole located at the image plane of the sample. In experiments, the requirements on this sampling dimension depend on the type of the experiment one performs. A larger scattering volume can be selected to enhance the signal intensity if the sample structure is uniform and the requirement on angular resolution not too high. In our experiments on the

smectic A phase in TMV solutions, it was desirable to have a sampling volume of about 100-200 $\mu$m and a good angular resolution for measuring the angular width of the Bragg diffractions. For this reason, 250-$\mu$m-wide pinholes were used in the modular pieces. The dimension of the sampling volume in our setup was measured by monitoring the decrease in the scattering intensity as the grating is moved away from the center of the scattering sphere while the detector is fixed at the maximum diffraction angle. From the intensity distribution illustrated in Fig. 2, a sampling dimension of about 130 $\mu$m is obtained. Since the Bragg geometry was slightly changed as the grating was displaced, this dimension also reflects some angular selection by the second pinhole in the third modular piece. The repeatabilities in the angular positions of the detector were found to be very good; the scattering signals at one angle do not change after a few forward and reverse runs in the entire ranges of both angular directions [Figs. 1(b) and 1(c)]. The detection arm and the sample were also found to be stable. No significant vibrations were observed.

In Figs. 3(a) and 3(b), we show the azimuthal and polar intensity distributions of the Bragg scattering from the smectic layers formed in TMV solutions. The sample was illuminated by a He-Ne laser with a wavelength of 6328 Å. The angle of the maximum diffraction in Fig. 3(a) corresponds to a layer spacing of 3329 Å. To test the remaining refractive effect at the walls of the cylindrical-shaped sample capillary, different sample volumes were selected at each fixed section along the capillary axis. The variation in layer spacing thus obtained was found to be within 1–2 Å. Using the angular resolution of 0.19°, we found from the angular widths in Figs. 3(a) and 3(b) that the smectic layer correlation lengths are much longer than 200 $\mu$m in the layer normal direction and about 60 $\mu$m parallel to the layers.[11]

This setup has also been applied to studying the quasielastic light scattering from hydrodynamic fluctuations in the TMV smectic A phase. Polarized and depolarized dynamic scattering were selected using the polarizer at the entrance end of the detection tube. The relaxation times of the hydrodynamic modes have been found to be consistent with theoretical predictions.[12]

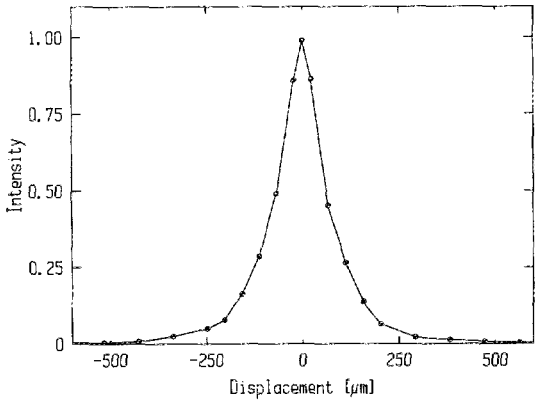


FIG. 2. The scattering intensity as a function of the displacement of the grating from the center of the scattering sphere. The detector was fixed at the angle where the maximum diffraction was measured. The circles are experimental data and the solid line is an aid to the eye.

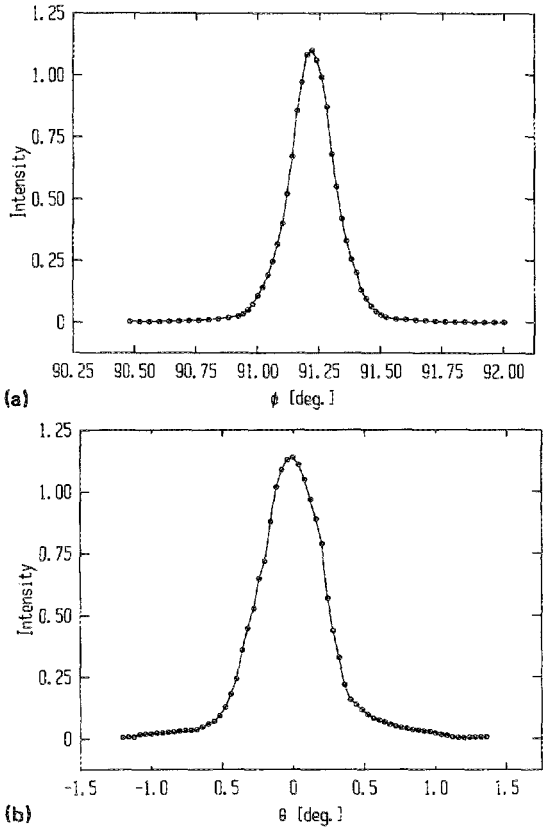


FIG. 3. The Bragg intensity distributions along (a) azimuthal and (b) polar directions, which is obtained from the layered liquid crystalline phase formed in solutions of tobacco mosaic virus. The sample was illuminated by an He-Ne laser beam with a wavelength 6328 Å and the layer normal was kept in a horizontal plane. The measurements were made by scanning the detector at an angular increment of 0.04° while the sample was fixed at the Bragg geometry. In Fig. 3(a), the scanning plane is kept horizontal and parallel to the reciprocal vector of the smectic layers. $\phi$ is the angle between the incident and scattering wavevectors. In Fig. 3(b), the scanning plane is perpendicular to that in Fig. 3(a). $\theta$ is the angle between the Bragg maximum direction and the scattering direction. The circles are experimental data and the solid line is an aid to the eye.

## ACKNOWLEDGMENTS

We would like to thank Xiaolei Ao for improvements in the detector and testing of the system, and Rudolf Oldenbourg and Frank Lonberg for helpful discussions. This project was supported in part by the National Science Foundation through Grant No. DMR88-03582, and by the Martin Fisher School of Physics at Brandeis University.

[1] B. Chu, *Laser Light Scattering* (Academic, New York, 1974).
[2] B. J. Berne and R. Pecora, *Dynamic Light Scattering: With Applications to Chemistry, Biology, and Physics* (Wiley, New York, 1976).
[3] F. Chang, H. Burstyn, and J. V. Sengers, Phys. Rev. A **29**, 866 (1979).
[4] H. R. Haller, C. Destor, and D. S. Cannell, Rev. Sci. Instrum. **54**, 973 (1983).
[5] F. C. Chen, A. Yeh, and B. Chu, J. Chem. Phys. **66**, 1290 (1977).
[6] J. S. Huang and M. W. Kim, in *Scattering Techniques Applied to Supermolecular and Nonequilibrium Systems*, edited by S. H. Chen, B. Chu, and R. Nossal (Plenum, New York, 1981), p. 831.
[7] A. M. Ganz and B. E. Boeger, Rev. Sci. Instrum. **56**, 2004 (1985).
[8] H. R. Haller, J. Phys. E **14**, 1137 (1981).
[9] H. Guttinger, J. H. Bilgram, and W. Kanzig, J. Phys. Chem. Solids **40**, 55 (1979).
[10] V. G. Taratuta, A. J. Hurd and R. B. Meyer, Rev. Sci. Instrum. **55**, 751 (1984).
[11] X. Wen, R. B. Meyer, and D. L. D. Caspar, Phys. Rev. Lett. **63**, 2760 (1989).
[12] X. Ao *et al.* (to be published).